Formation Kinetics and Structural Features of Beta-Amyloid Aggregates by Sedimented Solute NMR

DOI: 10.1002/cbic.200((will be filled in by the editorial staff))

SED-NMR for Beta Amyloid

Formation Kinetics and Structural Features of Beta-Amyloid Aggregates by Sedimented Solute NMR

Ivano Bertini[a,b,c,‡], Gianluca Gallo[a,d], Magdalena Korsak[a,b], Claudio Luchinat*[a,c,d], Jiafei Mao[a,c,†], Enrico Ravera[a,d]

Dedicated to Prof. Dr. Ivano Bertini (1940-2012): his brilliant mind and motivating spirit shine in this work and will continue to inspire us for many years to come.

The accumulation of soluble toxic beta-amyloid (Aβ) aggregates is an attractive hypothesis for the role of this peptide in the pathology of Alzheimer's Disease (AD). We have introduced sedimentation via ultracentrifugation, either by magic angle spinning (in situ) or preparative ultracentrifuge (ex situ), to immobilize biomolecules and make them amenable for solid-state NMR (SSNMR) studies (SedNMR). In situ SedNMR is used here to address the kinetics of formation of soluble Aβ assemblies by monitoring the disappearance of the monomer and the appearance of the oligomers at the same time. Ex situ SedNMR allows us to select different oligomeric species and to reveal atomic-level structural features of soluble Aβ assemblies.

Introduction

We have developed a method, termed Sedimented Solutes NMR (SedNMR) to observe by solid-state NMR experiments proteins that are sedimented from their solution by an ultracentrifugal field.[1-7] In concentrated protein solutions rotational diffusion is restricted by self-crowding.[8] SedNMR relies on the extreme concentration of the sediment[3;9;10] to make the protein appear solid on the MAS timescale and observable *via* SSNMR. Sedimentation of macromolecules into such a solid-like phase can be achieved in two ways:

a) direct *in situ* sedimentation by the magic-angle-spinning (MAS) of the NMR rotor that acts as an ultracentrifuge[1] (or MAS-induced sedimentation[3], left panel in figure 1) or

b) *ex situ* sedimentation by common ultracentrifuge[3-5] with the help of devices previously designed to pack NMR rotors with precipitates or microcrystals[11] (or UC-induced sedimentation[3], right panel in figure 1).

Previous theoretical calculations as well as experimental evidence have shown that proteins or protein complexes with molecular weight above 30 kDa could be efficiently sedimented.[1;3] *In situ* SedNMR has been demonstrated on ferritin,[1] bovine serum albumin and carbonic anhydrase,[3] and already applied to the study of αB-crystallin dynamics[12] and reactivity.[13] *Ex situ* SedNMR has beeen already applied to ferritin[3] and to a dodecameric helicase.[5]

Aβ aggregates show marked synaptotoxicity and neurotoxicity in both isolated neuronal cells and animal models and are therefore believed to be pathologically relevant in Alzheimer's disease (AD)[14-16]. From the recent literature these species show significant morphological and structural diversities and exert varied toxic effects.[17-20] Therefore high-resolution structural characterization of Aβ aggregates is of primary importance to understand the complex molecular mechanisms of AD[16]. We propose that in situ or ex situ SedNMR can be used to characterize oligomeric species, measure their formation kinetics, and even selectively sediment some of them by virtue of their different molecular weights.

Different structural models of mature Aβ fibrils have been proposed in several recent solid-state NMR (SSNMR) works[21-24]. Residue-specific information on prefibrillar Aβ aggregates (e.g oligomers and protofibrils) and on structural persistence in the

[a] *Prof. Dr. I. Bertini, Mr. G. Gallo, Ms. M. Korsak, Prof. C. Luchinat, Dr. J. Mao, Dr. E. Ravera*
Magnetic resonance Center (CERM),
University of Florence
Via L. Sacconi 6, 50019 Sesto Fiorentino, Italy
Fax: (+39) 055 457 4271
E-mail: claudioluchinat@cerm.unifi.it

[b] *Prof. Dr. I. Bertini, Ms. M. Korsak*
Giotto Biotech
Via Madonna del Piano 6, 50019 Sesto Fiorentino, Italy

[c] *Prof. Dr. I. Bertini, Prof. C. Luchinat, Dr. J. Mao*
Fondazione Farmacogenomica FiorGen onlus
Via L. Sacconi 6, 50019 Sesto Fiorentino, Italy

[d] *Prof. C. Luchinat, Mr. G. Gallo, Dr. E. Ravera*
Department of Chemistry "Ugo Schiff",
University of Florence
Via della Lastruccia 3, 50019 Sesto Fiorentino, Italy

[†] *Dr. J. Mao currently at Goethe Universität, Max-von-Laue-Str. 9, Biozentrum N202 60438 Frankfurt am Main.*

[‡] *Prof. Dr. I. Bertini passed away on July 7th 2012*

Supporting information for this article is available on the WWW under http://www.chembiochem.org or from the author

monomer has also been obtained through various experimental and theoretical methods. [15;17;20;25-32] However, prefibrillar assemblies are often unstable compared to mature fibrils, and therefore they cannot be trapped easily unless dehydration[28], organic solvents[32] or interaction partners[15;33;34] are introduced in the sample preparation. To date, characterization of prefibrillar Aβ aggregates in pure aqueous environment is still very challenging.[35] In pioneering works by the groups of Smith and Ishii, SSNMR characterization of Aβ oligomeric states in the lyophilized state were obtained and showed that the arrangement of the peptide was mainly β-sheet[25][28].

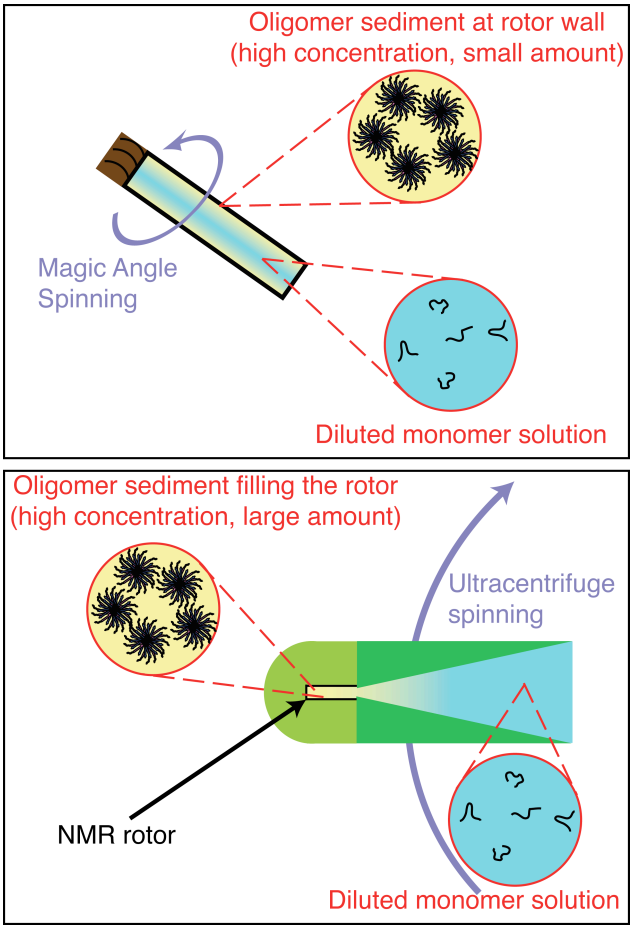

Figure 1. Pictorial representation of the process of sedimentation. In MAS-induced sedimentation (top) the sediment is created in a thin layer at the rotor walls (width of the sediment layer is greatly exaggerated). UC-induced sedimentation (bottom) can be used to effectively fill the rotor with sediment.

It has been reported [20;28;29;36;37] that in aqueous solutions Aβ peptides spontaneously form soluble aggregates of high molecular weight (50-200 kDa). These species should be massive enough to sediment and thus become visible by SSNMR. Here we show that this is indeed the case, and that aggregates of different molecular weights can be selectively obtained by changing the experimental conditions.

Results and Discussion

Kinetics determination via *in situ* SedNMR

Freshly prepared solutions of Met-0 Aβ40 peptide (AβM40) (160 μmol dm^{-3}) have been analyzed by solution NMR at 280 K. The free, intrinsically disordered Aβ monomer (4.6 kDa) is always the only component in the NMR spectra of the fresh samples. The disappearence of the sofastHMQC[38] signal was used to monitor aggregation. Consistently with what observed by Pauwels et al.,[39] the signal of the monomer persists for long time in the unagitated solution. After scratching the sample with a glass rod, the signal of the monomer started to decrease with a time dependence that appears as an exponential decay after an induction time (Fig. S1).

In the *in situ* SedNMR setup, the ^{13}C signals of free monomers and sedimented aggregates of AβM40 can be monitored using different ^{1}H-^{13}C polarization transfer methods: the solution part (i.e.: having τ_c of the order of tenths of ns, containing the monomer and possibly aggregates with MW < 60 kDa) can be excited through the J-coupling based Insensitive Nuclei Enhancement by Polarization Transfer (INEPT[40]) and detected under low power ^{1}H decoupling (2.5 kHz) or no decoupling at all [41;42]; the dipolar-based cross-polarization (CP[43]) can be used to excite the solid part that results immobilized on the MAS timescale (i.e.: having τ_c longer than the MAS period)[1;44]. When freshly prepared and concentrated AβM40 solutions are introduced in the SSNMR rotor, only the INEPT signal is visible (Figure S2). After applying MAS for some time the intensity of the INEPT signal decreases in favor of the growth of the CP signal (Figure 2).

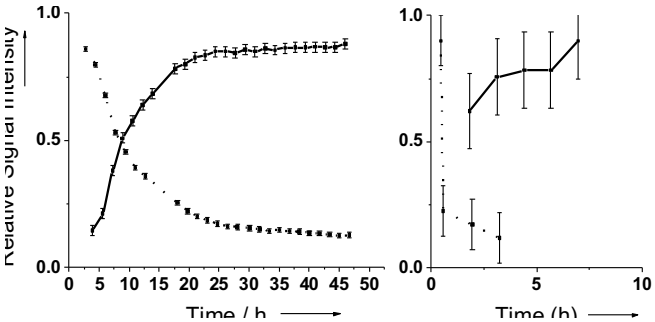

Figure 2. Relative signal intensity of INEPT (dashed) and CP (solid) signals for AβM40 (left) and AβM42 (right) as a function of time at 12 kHz spinning and 277 K.

We have quantitated the relative contribution of the solution part and of the solid part as a function of time. An 8 mmol dm^{-3} AβM40 solution was sealed in a 4.0 mm solid state NMR rotor (internal radius 1.5 mm) and spun at 12 kHz over 3 days, during which period interweaved INEPT and CP spectra were recorded. The intensities of the solution and solid signals are plotted in Figure 2 (left) dashed and solid, respectively. Data processing is described in the supporting information. By the use of equation 3 in reference[3], it is possible to calculate that the sediment observed under these conditions contains species with molecular weight above 70 kDa, as calculated for a MAS rate of 12 kHz (see supporting information). Aggregates of this MW would be expected to sediment completely in about 3 h (see supporting information), while Figure 2 (left) shows that the process is not completed until about 30 h. Therefore the formation of these aggregates is significantly slower than their sedimentation: thus, aggregates form slowly, and clean information about the kinetics is obtained. This physical picture is summarized in figure 3. It is also important to notice that the 1D ^{13}C CP spectra do not change significantly with time (Figure S3).

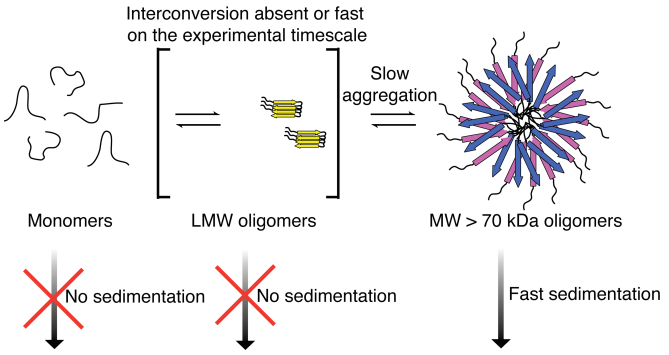

Figure 3. The physical picture underlying the kinetic determination: monomers and low molecular weight oligomers are too small to sediment. Their interconversion into larger oligomers is slow on the experimental timescale, thus they are the only contribution to the solution NMR signal. Larger oligomers are sedimented as soon as they are formed, thus they are the only contribution to the solid state NMR signal. The quaternary structures shown only reflect morphologies reported in the literature.

On the basis of these data, kinetic information is obtained on oligomer formation, and thanks to ultracentrifugation these species are trapped and prevented from changing. The kinetic behavior of this sample is consistent with what previously reported by Lee et al. [37], given the differences in construct, temperature, and initial monomer concentration. To obtain an independent validation of our approach, the same experiment was performed on an AβM42 sample at 0.8 mmol dm^{-3} concentration. In this case the aggregation is significantly faster (half-time of less than 1 h, Figure 2 (right)), consistently with the known behavior of the Aβ42 isoform.[39;45;46] This observation confirms that the much slower kinetics observed in the case of the AβM40 species is not due to the sedimentation of the oligomers but truly reflects their formation (figure 3). By the same token, we can conclude that for AβM42 a detailed analysis is prevented by formation and sedimentation possibly occurring on similar timescales. Data are plotted in Figure 2 (right) as solid (CP) and dashed (INEPT) lines.

Summarizing, species above 70 kDa will be observed by CP, while those below will be observed via INEPT. The fact that the relative intensities of the two signals sum to about 1 throughout the time course of the experiment shows that intermediate species that are invisible both by solution and by SSNMR are not formed to appreciable amount. Further discussion is given in the supporting information.

Sedimentation is much more efficient on large Aβ aggregates than on small Aβ monomers: in the experimental conditions applied here for MAS-induced sedimentation the monomer is not forming an appreciable concentration gradient. Therefore sedimentation has the ability to separate the soluble aggregates from the bulk solution, and drive the equilibrium towards the oligomeric species.[7;47] Obviously if a small amount of large aggregates is already present, it will sediment along with the forming small species. However, in this case, the presence of significant amounts of large aggregates can be excluded, given that no solid state NMR signal is observed at all at the beginning of the experiment.

It is to be noted that formation of fibrils is a highly anisotropic phenomenon, requiring aggregation in (mainly) only one dimension. While this is easily attained in the classical fibrillation approaches [23;24;48;49], we may expect that this process can be hindered by the strongly impaired rotation of the oligomeric species once they are sedimented. Minton and Ellis have predicted using scaled particle theory that aggregation is made faster by macromolecular crowding,[50] and experimental verification was provided by White et al..[51] Our hypothesis is in line with coarse-grained calculations by Magno et al.[52] suggesting that crowding will increase the oligomerization kinetics preventing at the same time the formation of fibrils. This means that a sedimented sample could be rendered inert, and prefibrillar Aβ aggregates may be stabilized in such a phase.

The impact of self-crowding on the aggregation kinetics may not be trivial: the oligomers increase in concentration, thus they can extend by binding the free monomers. The aggregation kinetics will be thus accelerated by the increase of the concentration of one reagent. Anyway, two major aspects must be considered:

a) the tight packing of the oligomers at the rotor walls will prevent diffusion of the species, thus at some point of the process the solution will be devoid of free monomers, and successive aggregation will be hindered;

b) the concentration of the oligomers is increased in a limited amount of space, thus the bulk monomer will not sense any increase in the oligomer content.

c) the oligomers are subtracted from the bulk, thus they cannot function as seeds[53] for further aggregation.

The overall effect on the measured kinetics is the following (shown in Figure S1): aggregation is made faster with respect to the unagitated solution (half time is reduced approximately of a factor 4) and the kinetics appears more monoexponential, consistently with point (c). It is possible to monitor disappearance of the monomer by normal solution experiments (see Figure S1), but it is important to notice that only the comparison with the cross polarization signal is able to reveal in full the kinetic properties of the system. In summary, MAS-induced sedimentation can be a simple but useful tool to monitor the kinetics of formation of the prefibrillar Aβ aggregates, especially by comparing different preparations, reducing the possible bias arising from MAS.

Structural features via *ex situ* SedNMR

A 2D ^{13}C-^{13}C correlation spectrum was recorded on the MAS-induced sediment. The appearance of the spectrum of the oligomers in the MAS-induced sediment suggests that elements of beta structure are present (Figure S5). In the following section we wish to demonstrate that structural information can be extracted from SS-NMR spectra of sedimented samples. In the above described MAS induced sedimentation experiment, all prefibrillar aggregates with MW higher than 70 kDa that may be present in the solution are collected into sediment and cannot be distinguished. On the contrary, UC-induced sedimentation[3-5] selection on the basis of the ultracentrifugation time is possible, and fractional centrifugation (a classical ultracentrifuge preparation) can be also used to differentiate fractions of different molecular weight. An approach based on fractional centrifugation was successfully applied on soluble oligomers of α-synuclein, and SSNMR spectra were acquired in the frozen state.[54] In line with this, we applied UC-induced sedimentation to AβM40 preparations under different conditions. Conditions and samples are listed in table 1.

Taking into account the time during which sedimentation was performed, the molecular weight limit is dictated by the integrated Svedberg equation[55] to about 70 kDa in samples UC-1 and UC-2, and to 140 kDa for sample UC-3 (see supporting information).

Table 1. Condition for preparation of UC-induced samples

Sample	Initial AβM40 concentration (mmol dm^{-3})	Ultracentrifugation frequency [a] (rpm)	Ultracentrifugation time (h)	Calculated lower limit of MW to sediment (kDa)
UC-1	1.4	32 000	24	70
UC-2	10.0	32 000	24	70
UC-3	1.4	15 000	72	150

[a] In a Beckman Coulter Optima L80K floor preparative ultracentrifuge using a SW32 rotor

A priori control over the observed species in a MAS induced sedimentation experiment on prefibrillar aggregates is not possible: to achieve sufficient averaging of anisotropic interactions, MAS should be operated at a frequency that provides centrifugal accelerations larger than what is normally done in an ultracentrifuge. This reduces the possibility of differentiating between high molecular weight components, and fractional centrifugation is unpractical in the closed rotor.

For the sample manipulations reported in Table 1, by numerical integration of equation 3 of reference[3] the lowest molecular weight of the sedimenting material should be of the order of 20 kDa,[4;29] (see supporting information). The value of 70 kDa for sample UC-1 is in agreement with the value observed in its native gel, as shown in Fig. 4. Bands of oligomeric AβM40 with MW of 69 kDa (15-mer), 138 kDa (30-mer) and 207 kDa (45-mer) have been observed. Oligomer bands have not been found in the native gel of the UC-2 sample but the bands of monomers as well as SDS-stable dimers and tetramers have been detected from SDS-PAGE analysis of this sample, suggesting that larger assemblies can form at high initial monomer concentration.[56]

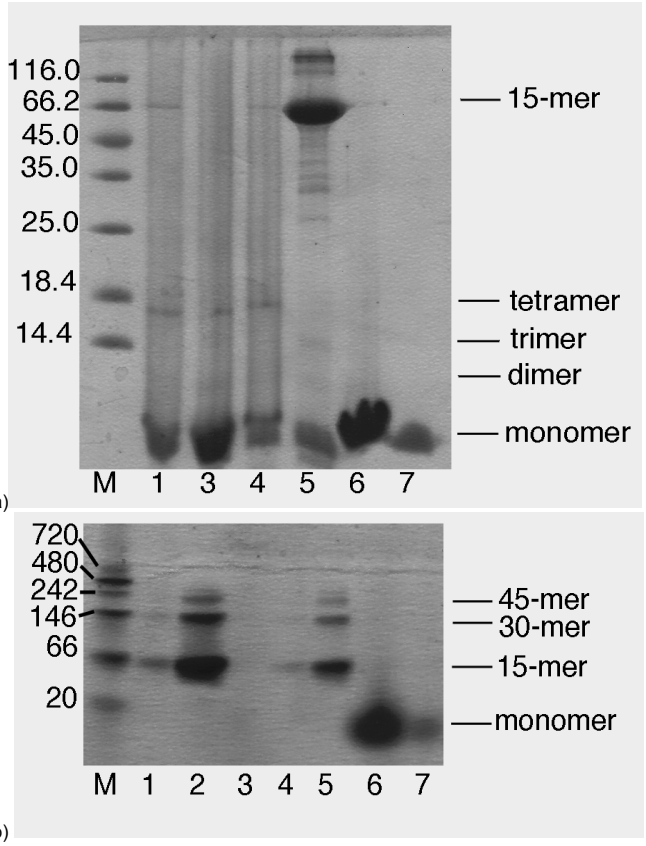

Figure 4. a) SDS-PAGE showing the apparent mass of SDS-resistant species; samples are in the order: M – Marker, 1 – UC-induced at 1.4 mmol dm^{-3}, 3 – UC-induced sediment at 10 mmol dm^{-3}, 4 – MAS-induced sediment at 8 mmol dm^{-3}, 5 – MAS-induced sediment at 2 mmol dm^{-3}, 6 – supernatant from the preparation of sample 1-2, 7 – monomer. The tetramer band (18 kDa) is evident in samples 1,3,4 , while the sample 5 shows the marked presence of heavier species as 68 kDa and approximately 146 kDa. b) Native gel electrophoresis showing the apparent mass of oligomers; samples are in the order: M – Marker, 1 and 2 – UC-induced at 1.4 mmol dm^{-3}, 3 – UC-induced sediment at 10 mmol dm^{-3}, 4 – MAS-induced sediment at 8 mmol dm^{-3}, 5 – MAS-induced sediment at 2 mmol dm^{-3}, 6 – supernatant from the preparation of sample 1-2, 7 – monomer. The most abundant species in samples 1,2 and 4,5 is the 68 kDa oligomer (15-mer), in agreement with the theoretical predictions, with other two major bands at about 146 and 207, consistent with the 30-mer and 45-mer respectively. In sample 3 no soluble specie is observed.

Sample UC-1 was analyzed through dipolar-coupling based ^{13}C-^{13}C 2D SHANGHAI[57] spectra and ^{15}N-^{13}C correlation spectra (NCA/NCO[58], shown in figure S4). Spectra have lines of the order of 80 Hz at 850 MHz and 100 Hz at 700 MHz for the Isoleucine 31 Cγ1 signal (Figure 6). As expected, samples UC-2 and UC-3, likely to contain a larger distribution of species and larger species, respectively, yielded less resolved spectra, as reported in figure S5. In the case of UC-2 this may be due to large inhomogeneity of the oligomer sizes due to high concentration: as seen in gel electrophoresis (Fig. 4), larger species might be formed at high initial concentration. In the case of UC-3 the lower resolution is probably due to a larger spread of oligomer sizes at the high end, given the longer time during which the sample is allowed to aggregate.

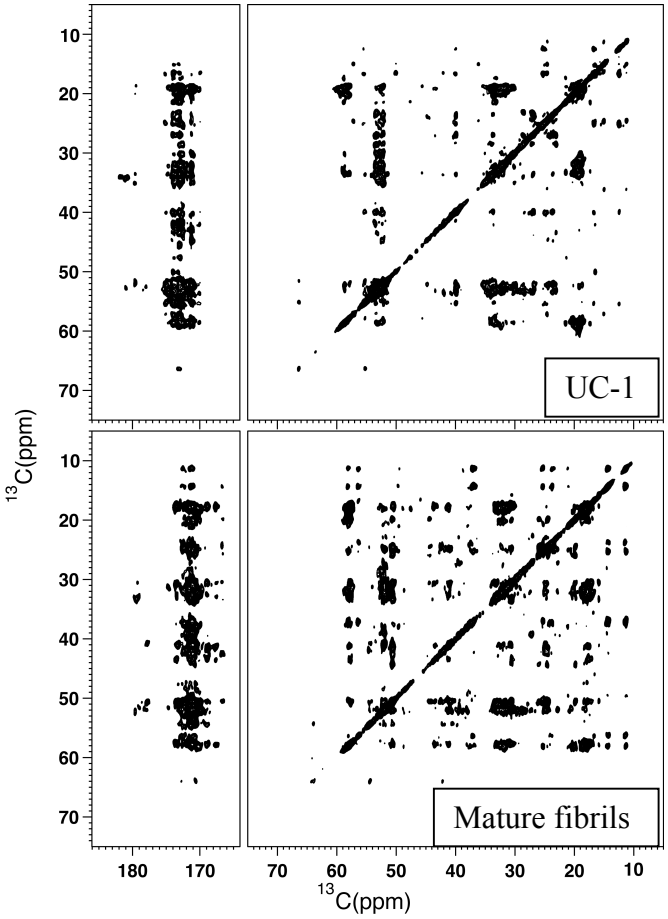

Figure 5. Comparison of the 300 ms ^{13}C-^{13}C-SHANGHAI spectrum of the UC-1 sample (top) and of the mature fibrils[23] (bottom).

Noticeably, the mixing times required for obtaining connectivities in sample UC-1 are rather long, as compared for instance to the mature fibrils,[23] suggesting that quite large mobility is present in the aggregates. An explanation for this may be that disordered oligomers[59] are subjected to compaction due to the self-crowding induced by sedimentation, but only a non completely compact state is achieved. For the larger species expected in samples UC-2 and UC-3 the supramolecular organization is expected to be more stable, converging to what is observed in the mature fibrils, and the same mixing times yield richer patterns.

The sharp lines and relative paucity of the peaks in sample UC-1 suggest a significant degree of order. For samples UC-2 and UC-3 likely containing a larger spread of MW, the order progressively decreases and the spectra become progressively broader.

It is also important to note that, in the SSNMR rotor, the formation of the sediment is reversible for concentrations as high as 5 mmol dm^{-3}, while it becomes irreversible at higher concentrations. In the case of the UC-induced sediment, the reversibility, also in the absence of further aggregation, is intrinsically limited by the ratio of the surface exposed to the solvent and the volume of the sediment[3].

Apparently, all the peaks appearing in the ^{13}C-^{13}C 2D SHANGHAI spectrum of the MAS-induced sediment (red in figure S6) are maintained in the corresponding spectrum recorded on the UC-1 sample (green in figure S6). This suggests that similar species are formed and observed in the two experiments. In the latter case, the higher signal to noise ratio, probably combined with a larger compaction, allowed for detection of a larger number of weaker crosspeaks, while the resolution is not compromised. On the other hand, as shown in figure 5, the ^{13}C-^{13}C 2D SHANGHAI spectrum of UC-1 is not superimposable to the corresponding spectrum of mature Aβ fibrils prepared in the same solution condition[23]. The UC-1 sample was stable throughout the full spectroscopic characterization.

A partial sequential assignment was obtained, taking advantage of the high resolution and adequate sensitivity of the 2D spectra on the UC-1 samples as well as of the short and simple sequence pattern of the Aβ peptide. The intensity and resolution of the peaks in the Cα region (see figure 5) allowed for recognition of Cα - Cα and Cα - CX crosspeaks between neighboring residues in the 2D ^{13}C-^{13}C SHANGHAI spectra, and these connectivities were followed in order to achieve a sequential walk passing from Lys16 to Gly38, as exemplified in figure S7, and comparing the shifts with the expected aminoacid-specific values. We have found that only one set of chemical shifts as reported in Table S1 can explain all these sequential/short range contacts and no signal doubling has been observed with the exception of I31. For this residue (cross-hatched in figure 6), more than one set of resonances have been observed. This indicates conformational heterogeneity in the turn region near the β2 element. No sequential connectivity was found for residues 1-15, consistently with an increased mobility in this region, as already observed in many fibrillar preparations.

Based on these backbone chemical shifts, some structural features of these aggregates can be obtained on this sample. Such observations, described below, are summarized in figures 6 and 7. We recall that this sample is in a fully hydrated and free state, without the addition of interacting molecules, and that no structural information has been made available so far for such a sample.

The secondary chemical shifts indicate that the most hydrophobic parts (mostly residues 16-22 and, to a minor extent, residues 30-38) of the AβM40 peptide already form β-strands in the present oligomeric species. This observation is consistent with that proposed based on recent DEST studies on Aβ prefibrillar aggregates[29]. Figure S9 reports the PREDITOR[60] and TALOS[61] prediction of the backbone dihedral angles calculated through the WeNMR web interfaces[62]. Both programs predict extended beta secondary structures, and PREDITOR also pinpoints a break in the beta-stretch between residues 23 and 30.These stretches are within the longer β1- and β2-regions in mature fibrils (10-22 and 26-38), indicating that expansion of these two “nascent” β-strands is possibly one of the main events during Aβ fibril maturation. This is also consistent with what previously proposed by other groups based on the observation of samples trapped in the oligomeric states by different approaches.[15;25;28;63] The signals of residues 39 and 40 are not found. This is consistent with the increased mobility of these residues previously reported on antibody-stabilized protofibrils[15]. Moreover, the β-propensities of these two residues are slightly decreased compared to the central region of the β2 strand in mature fibrils[23]. This suggests that such structural differences within mature fibrils originate already from the prefibrillar stage. S26 is also found to have a high chemical shift perturbation and we were able to assign crosspeaks consistent with a salt bridge being present between E22 and K28 (green line in figure 8, spectrum in figure S8). Such interaction would decrease the mobility of the loop and justify the large chemical

shift perturbation of S26. Crosspeaks in the crowded region around (δ_1, δ_2)=(20 ppm,55 ppm) that can be ambiguously attributed to contacts (L17,V18)-(L34,M35) (dashed lines in figure 6) are also observed. These contacts may be consistent with arrangements typical of mature fibrils (in a form of mature fibrils, a similar register was observed by Tycko and coworkers[49;64]), or with a β-hairpin arrangement. The latter has been observed by Sandberg et al.[59] in complex with an affibody binding protein.

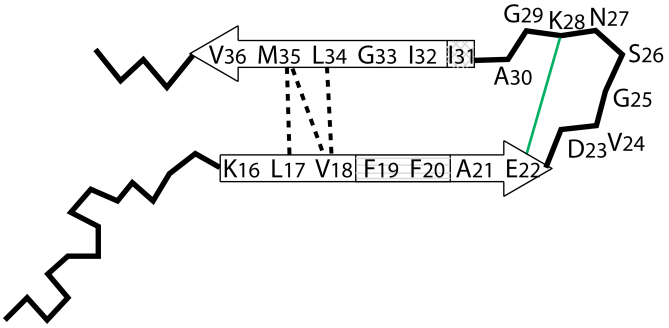

Figure 6. Schematics of the structural information obtained for Aβ oligomers. The preformed secondary structure elements, based on the PREDITOR prediction, are reported as red arrows. F19 and F20 are line-hatched because the side chain resonances cannot be distinguished. I31 is cross-hatched to highlight its structural heterogeneity. The unambiguous contact between E22 and K28 is reported as a solid line, whereas the ambiguous contacts contacts (L17,V18)-(L34,M35) are reported as dashed lines.

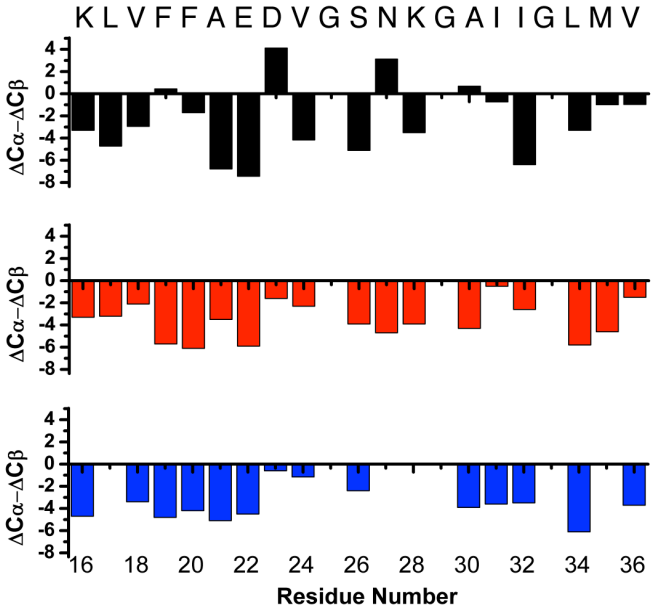

Figure 7. NMR observables as predictors for secondary structure content for the oligomers (top panel): β structure of regions 16-22 and 32-36 can be inferred. Comparison is made to the mature fibrils[23] (middle panel) and to oligomers stabilized in the presence of HFIP[32] (lower panel). Glycines are not shown.

Conclusions

In conclusion we have shown that SedNMR allows for collecting and trapping of AβM40 aggregates in fully hydrated environment without adding cosolvents or interaction partners, and therefore provides a unique way to access the formation kinetics and structural features of these species with reduced perturbations. With a minimal sample preparation we have probed the kinetics of aggregation of the AβM40 peptide. This piece of information is validated by the comparison with the faster aggregating AβM42. A similar form of the prefibrillar AβM40 aggregates, obtained by sedimentation in a preparative ultracentrifuge, was analyzed to obtain a qualitative picture of its structural features. This approach can be easily applied to other amyloid systems and more generally to the study of many supramolecular assembly processes.

Acknowledgements

Discussions with Gary J. Pielak on crowding effects and with Yoshitaka Ishii on Aβ reactivity during the Chianti/Instruct Workshop on BioNMR 2012 are acknowledged. We thank Marco Fragai for careful reading of the manuscript and for providing insightful suggestions. This work has been supported by the EC contracts East-NMR no. 228461 and Bio-NMR no. 261863, Ente Cassa Risparmio Firenze, and INSTRUCT, part of the European Strategy Forum on Research Infrastructures (ESFRI) and supported by national member subscriptions. Specifically, we thank the EU ESFRI Instruct Core Centre CERM Italy. MK acknowledges EC MC ITN IDPbyNMR Contract n° 264257 for financial support.

Keywords: ((centrifugation · oligomerization · sedimentation · ·kinetics · solid-state NMR spectroscopy))

[1.] I. Bertini, C. Luchinat, G. Parigi, E. Ravera, B. Reif, P. Turano, Proc.Natl.Acad.Sci.USA 2011, 108 10396-10399.
[2.] T. Polenova, Nature Chemistry 2011, 759-760.
[3.] I. Bertini, F. Engelke, C. Luchinat, G. Parigi, E. Ravera, C. Rosa, P. Turano, Phys.Chem.Chem.Phys. 2012, 14 439-447.
[4.] I. Bertini, F. Engelke, L. Gonnelli, B. Knott, C. Luchinat, D. Osen, E. Ravera, J.Biomol.NMR 2012, 54 123-127.
[5.] C. Gardiennet, A. K. Schütz, A. Hunkeler, B. Kunert, L. Terradot, A. Böckmann, B. H. Meier, Angew.Chem.Int.Ed 2012, 51 7855-7858.
[6.] E. Ravera, B. Corzilius, V. K. Michaelis, C. Rosa, R. G. Griffin, C. Luchinat, I. Bertini, J.Am.Chem.Soc. 2013, 135 1641-1644.
[7.] I. Bertini, C. Luchinat, G. Parigi, E. Ravera, Acc.Chem.Res. 2013, Epub ahead of print .
[8.] Y. Wang, C. Li, G. J. Pielak, JACS 2010, 132 9392-9397.
[9.] S. Lundh, Archives of Biochemistry and Biophysics 1985, 241 265-274.
[10.] S. Lundh, Journal of Polymer Science: Polymer Physics Edition 1980, 18 1963-1978.
[11.] A. Böckmann, C. Gardiennet, R. Verel, A. Hunkeler, A. Loquet, G. Pintacuda, L. Emsley, B. H. Meier, A. Lesage, J.Biomol.NMR 2009, 45 319-327.
[12.] A. J. Baldwin, P. Walsh, D. F. Hansen, G. R. Hilton, J. L. P. Benesch, S. Sharpe, L. E. Kay, J.Am.Chem.Soc. 2012, 134 15343-15350.
[13.] A. Mainz, B. Bardiaux, F. Kuppler, G. Multhaup, I. C. Felli, R. Pierattelli, B. Reif, J.Biol.Chem. 2012, 287 1128-1138.
[14.] N. Carulla, M. Zhou, E. Giralt, C. V. Robinson, C. M. Dobson, Acc.Chem.Res. 2010, 43 1072-1079.
[15.] H. A. Scheidt, I. Morgado, S. Rothemund, D. Huster, M. Fandrich, Angew.Chem.Int.Ed. 2011, 50 2837-2840.
[16.] I. Benilova, E. Karran, B. De Strooper, Nat.Neurosci. 2012, 15 1-9.
[17.] S. L. Gallion, Plos ONE 2012, 7 e49375.
[18.] R. Roychaudhuri, M. Yang, M. M. Hoshi, D. B. Teplow, J.Biol.Chem. 2009, 284 4749-4753.
[19.] G. Bitan, S. S. Vollers, D. B. Teplow, J.Biol.Chem. 2003, 278 34882-34889.
[20.] S. L. Bernstein, N. F. Dupuis, N. D. Lazo, T. Wyttenbach, M. M. Condron, G. Bitan, D. B. Teplow, J. E. Shea, B. T. Ruotolo, C. V. Robinson, M. T. Bowers, Nature Chem. 2009, 1 326-331.
[21.] M. Fandrich, M. Schmidt, N. Grigorieff, Trends in Biochemical Sciences 2011, 36 338-345.
[22.] R. Tycko, Annu.Rev.Phys.Chem. 2011, 62 x-xx.
[23.] I. Bertini, L. Gonnelli, C. Luchinat, J. Mao, A. Nesi, J.Am.Chem.Soc. 2011, 133 16013-16022.
[24.] J. M. Lopez del Amo, M. Schmidt, U. Fink, M. Dasari, M. Fändrich, B. Reif, Angew.Chem Int.Ed Engl. 2012, 51 6136-6139.
[25.] S. Chimon, Y. Ishii, J.Am.Chem.Soc. 2005, 127 13472-13473.
[26.] J. Danielsson, A. Andersson, J. Jarvet, A. Gräslund, Magn Reson.Chem. 2006, 44 S114-S121.

[27.] I. Kheterpal, M. Chen, K. D. Cook, R. Wetzel, J.Mol.Biol. 2006, 361 785-795.
[28.] M. Ahmed, J. Davis, D. Aucoin, T. Sato, S. Ahuja, S. Aimoto, J. I. Elliott, W. E. Van Nostrand, S. O. Smith, Nat.Struct.Mol.Biol. 2010, 17 561-567.
[29.] N. L. Fawzi, J. Ying, R. Ghirlando, D. A. Torchia, G. M. Clore, Nature 2011, 480 268-272.
[30.] J. Pan, J. Han, C. H. Borchers, L. Konermann, Anal.Chem. 2011, 83 5386-5393.
[31.] M. Fandrich, J Mol.Biol. 2012, 421 440.
[32.] C. Haupt, J. Leppert, R. Rönicke, J. Meinhardt, J. K. Yadav, R. Ramachandran, O. Ohlenschläger, K. G. Reymann, M. Görlach, M. Fandrich, Angew.Chem Int.Ed Engl. 2012, 51 1576-1579.
[33.] J. Bieschke, M. Herbst, T. Wiglenda, R. P. Friedrich, A. Boeddrich, F. Schiele, D. Kleckers, J. M. Lopez del Amo, B. A. Grüning, Q. Wang, M. R. Schmidt, R. Lurz, R. Anwyl, S. Schnoegl, M. Fandrich, R. F. Frank, B. Reif, S. Günther, D. M. Walsh, E. E. Wanker, Nat.Chem.Biol. 2012, 8 93-101.
[34.] J. M. Lopez del Amo, U. Fink, M. Dasari, G. Grelle, E. E. Wanker, J. Bieschke, B. Reif, J.Mol.Biol. 2012, 421 517-524.
[35.] J. C. Stroud, L. Cong, P. K. Teng, D. Eisenberg, Proc.Natl.Acad.Sci.USA 2012, 109 7717-7722.
[36.] M. D. Kirkitadze, G. Bitan, D. B. Teplow, J.of Neurosci.Res. 2002, 69 567-577.
[37.] J. Lee, E. K. Culyba, E. T. Powers, J. W. Kelly, Nat.Chem.Biol. 2011, 7 602-609.
[38.] P. Schanda, E. Kupce, B. Brutscher, J.Biomol.NMR 2005, 33 199-211.
[39.] K. Pauwels, T. L. Williams, K. L. Morris, W. Jonkheere, A. Vandersteen, G. Kelly, J. Schymkowitz, F. Rousseau, A. Pastore, L. C. Serpell, K. Broersen, J.Biol.Chem. 2012, 287 5650-5660.
[40.] G. A. Morris, R. Freeman, J.Am.Chem.Soc. 1979, 101 760-762.
[41.] W. Bermel, I. Bertini, I. C. Felli, M. Piccioli, R. Pierattelli, Progr.NMR Spectrosc. 2006, 48 25-45.
[42.] R. Riek, G. Wider, K. Pervushin, K. Wüthrich, Proc.Natl.Acad.Sci.USA 1999, 96 4918-4923.
[43.] A. Pines, M. G. Gibby, J. S. Waugh, J Chem Phys 1972, 56 1776-1777.
[44.] A. Mainz, S. Jehle, B. J. van Rossum, H. Oschkinat, B. Reif, J.Am.Chem.Soc. 2009, 131 15968-15969.
[45.] W. B. Jr. Stine, K. N. Dahlgren, G. A. Krafft, LaDu M.J., J Biol.Chem. 2003, 278 11612-11622.
[46.] I. Kuperstein, K. Broersen, I. Benilova, J. Rozenski, W. Jonekheere, M. Debulpaep, A. Vandersteen, I. Segers-Nolten, K. Van der Werf, V. Subramaniam, D. Braeken, G. Callewaert, C. Bartic, R. D'Hooge, I. C. Martins, F. Rousseau, J. Schymkowitz, B. De Strooper, EMBO J. 2010, 29 3408-3420.
[47.] R. C. Chatelier, A. P. Minton, Biopolymers 1987, 26 507-524.
[48.] A. T. Petkova, R. D. Leapman, Z. H. Guo, W. M. Yau, M. P. Mattson, R. Tycko, Science 2005, 307 262-265.
[49.] A. K. Paravastu, R. D. Leapman, W. M. Yau, R. Tycko, Proc.Natl.Acad.Sci.USA 2008, 105 18349-18354.
[50.] R. J. Ellis, A. P. Minton, Biological Chemistry 2006, 387 485-497.
[51.] D. A. White, A. K. Buell, T. P. J. Knowles, M. E. Welland, C. M. Dobson, J.Am.Chem.Soc. 2010, 132 5170-5175.
[52.] A. Magno, A. Caflisch, R. Pellarin, J.Phys.Chem.Lett. 2010, 1 3027-3032.
[53.] T. P. J. Knowles, C. A. Waudby, G. L. Devlin, S. I. A. Cohen, A. Aguzzi, M. Vendruscolo, E. M. Terentjev, M. E. Welland, C. M. Dobson, Science 2009, 326 1533-1537.
[54.] H.-Y. Kim, M.-K. Cho, A. Kumar, E. Maier, C. Siebenhaar, S. Becker, C. O. Fernandez, H. A. Lashuel, R. Benz, A. Lange, M. Zweckstetter, J.Am.Chem.Soc. 2009, 131 17482-17489.
[55.] Y. F. Mok, G. J. Howlett, Methods In Enzymology 2006, 413 199-217.
[56.] D. Kashchiev, R. Cabriolu, S. Auer, J.Am.Chem.Soc. 2013, 135 1531-1539.
[57.] B. Hu, O. T. J. Lafon, Q. Chen, J.-P. Amoureux, Journal of Magnetic Resonance 2011, 212 320-329.
[58.] N. M. Loening, M. Bjerring, N. C. Nielsen, H. Oschkinat, Journal of Magnetic Resonance 2012, 214 81-90.
[59.] A. Sandberg, L. M. Luheshi, S. Sollvander, T. P. de Barros, B. Macao, T. P. J. Knowles, H. Biverstal, C. Lendel, F. Ekholm-Petterson, A. Dubnovitsky, L. Lannfelt, C. M. Dobson, T. Hard, Proceedings of the National Academy of Sciences of the United States of America 2010, 107 15595-15600.
[60.] M. V. Berjanskii, S. Neal, D. S. Wishart, Nucleic Acids Res. 2006, 34 W63-W69.
[61.] Y. Shen, F. Delaglio, G. Cornilescu, A. Bax, Journal of Biomolecular NMR 2009, 44 213-223.
[62.] T. A. Wassenaar, M. van Dijk, N. Loureiro-Ferreira, G. van der Schot, S. J. de Vries, C. Schmitz, J. van der Zwan, R. Boelens, A. Giachetti, L. Ferella, A. Rosato, I. Bertini, T. Herrmann, H. R. A. Jonker, A. Bagaria, V. Jaravine, P. Guntert, H. Schwalbe, W. F. Vranken, J. F. Doreleijers, G. Vriend, G. W. Vuister, D. Franke, A. Kikhney, D. I. Svergun, R. H. Fogh, J. Ionides, E. D. Laue, C. Spronk, S. Jurksa, M. Verlato, S. Badoer, S. Dal Pra, M. Mazzucato, E. Frizziero, A. M. J. J. Bonvin, Journal of Grid Computing 2012, 10 743-767.
[63.] S. Chimon, M. A. Shaibat, C. R. Jones, D. C. Calero, B. Aizezi, Y. Ishii, *Nature Structural & Molecular Biology* **2007,** *14* 1157-1164.
[64.] A. T. Petkova, W. M. Yau, R. Tycko, *Biochemistry* **2006,** *45* 498-512.

Received: ((will be filled in by the editorial staff))
Published online: ((will be filled in by the editorial staff))

Layout 2:

FULL PAPERS

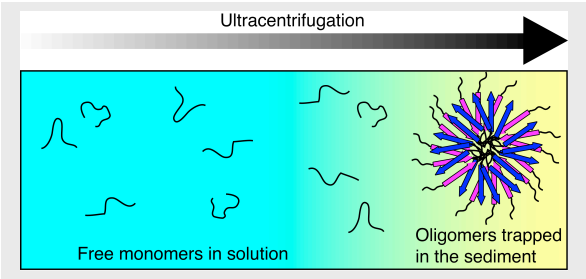

Ivano Bertini[a,b,c,‡], *Gianluca Gallo*[a,d], *Magdalena Korsak*[a,b], *Claudio Luchinat*[*a,c,d], *Jiafei Mao*[a,c,†], *Enrico Ravera*[a,d]

Page No. – Page No.

Formation Kinetics and Structural Features of Beta-Amyloid Aggregates by Sedimented Solute NMR

Formation Kinetics and Structural Features of Beta-Amyloid Aggregates by Sedimented Solute NMR

Ivano Bertini[a,b,c], *Gianluca Gallo*[a,d], *Magdalena Korsak*[a,b], *Claudio Luchinat*[*a,c,d], *Jiafei Mao*[a,c], *Enrico Ravera*[a,d]

[a]Magnetic resonance Center (CERM), University of Florence, Via L. Sacconi 6, 50019 Sesto Fiorentino, Italy

[b]Giotto Biotech, Via Madonna del Piano 6, 50019 Sesto Fiorentino

[c]Fondazione Farmacogenomica FiorGen onlus, Via L. Sacconi 6, 50019 Sesto Fiorentino,

[d]Department of Chemistry "Ugo Schiff", University of Florence, Via della Lastruccia 3, 50019 Sesto Fiorentino, Italy

Supporting Information

Protein expression and purification

The sample preparation was performed as previously reported[23]. The DNA encoding for beta amyloid peptide with methionine as first amino acid (AβM40) was cloned into a pET3a vector using *Nde*I and *Bam*HI restriction enzymes. BL21 (DE3) *Escherichia coli* cells were used for peptide expression. Cells were grown in LB rich medium at 37 °C until OD_{600} reached 0.8. The cells were then centrifuged and resuspended in minimal medium enriched with $(^{15}NH_4)_2SO_4$ (1 g/L) and [U-^{13}C]glucose (4 g/L). After 1 h 1mmol dm^{-3} isopropyl β-D-1-thiogalactopyranoside (IPTG) was added in order to induce the peptide expression. Cells were harvested after 4 h incubation at 39 °C, sonicated and ultracentifuged. Inclusion bodies were resuspended in 8 mol dm^{-3} urea and the peptide was purified by an anion exchange chromatography and a size-exclusion chromatography in 50 m mol dm^{-3} ammonium acetate (pH 8.5). In order to keep AβM40 in the monomeric form guanidinium chloride was added to a final concentration of 6 mol dm^{-3} before the last step of purification.

***Ex situ* sedimentation and estimation of the amount of sedimented material**

Ex situ sedimentation was performed at 4 °C in a Beckman Coulter Optima L80K floor preparative ultracentrifuge using a SW32 swinging bucket rotor using an ultracentrifugal device (University of Florence).[4] These preparations resulted in approximately 2.6 mg, 3.2 mg and 7.8 mg of sediment in the rotor respectively. Since the rotor contains also solution, the amount of protein in the rotor was not estimated by weighing but from the CP intensity with respect to the mature fibrils[23] (same CP conditions were used for this quantification).

Solid state NMR spectroscopy

Spectra were acquired on Bruker Avance II spectrometers operating either at 850 MHz or 700 MHz ^{1}H larmor frequency equipped with a 3.2 mm triple resonance probe (850) and 3.2 mm or 4 mm triple resonance probes (700).

Temperature was kept at 274 K (at sample) for the experiments acquired in the 3.2 mm rotors and at 277 K for the experiments acquired in the 4 mm rotors.

^{1}H excitation and decoupling nutation frequencies were 92.6 kHz in all cases.

^{13}C and ^{15}N 90° pulse lengths were 4.5 μs and 7.1 μs respectively, the ^{1}H, ^{13}C and ^{15}N carrier frequencies were set to 3.5 ppm, 90 ppm and 118 ppm, respectively.

The acquisition times in the SHANGHAI[57] experiment conducted at the 850 MHz spectrometer were 18 ms in the direct dimension and 3 ms in the indirect dimension.

The acquisition times in the SHANGHAI experiment conducted at the 700 MHz spectrometer were 19 ms in the direct dimension and 7 ms in the indirect dimension.

Interscan delay of 3.0 s was used and a different number of scans (from 160 to 256) in different experiments were accumulated for each t1 point.

The spectra were acquired using the States-TPPI mode. The spectra were processed with a 1024×4096 points matrix using squared cosine and gaussian window functions for the indirect and direct dimensions, respectively. Linear prediction with 12 coefficients was applied.

In the NCA and NCO conducted at the 700 MHz instrument, the ^{13}C carrier frequency was set to 54 ppm (NCA) or 172 ppm (NCO), and moved back to 90 ppm after the DCP. Optimal control pulses derived from Loening et al. were used[58]. Spectra were recorded with 544 scans (NCA) and 704 scans (NCO) per t1 increment. Acquisition times were 12 ms and 6 ms for the direct and indirect dimension respectively for NCA and 17 ms and 14 ms for the direct and indirect dimension respectively for NCO.

The spectra were acquired using the States-TPPI mode. The spectra were processed with a 256×4096 points matrix using squared cosine and gaussian window functions for the indirect and direct dimensions, respectively. Linear prediction with 8 coefficients was applied.

Figure S1 – Kinetics of disappearance of Aβ monomer from solution.

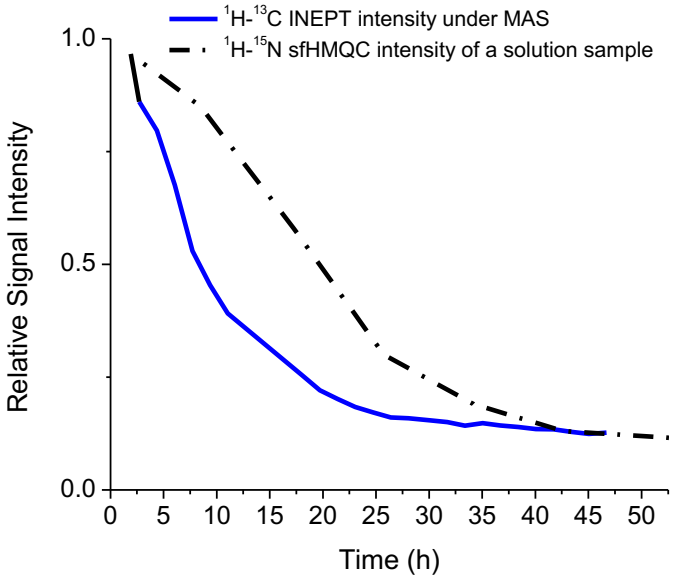

The diagram shows the signal intensity of the solution component of two AβM40 samples. Blue, solid line: the ^{1}H-^{13}C INEPT signal intensity observed for a 1.6 mM solution at 275 K, sealed in a 4 mm MAS rotor and spun at 12 kHz. Frictional heating can be estimated to be around 10 K. Black, dashed line: ^{1}H-^{15}N sfHMQC signal intensity (observed as a trace in the sidechains region in the 2D spectrum) for a 0.16 mM sample at 298 K after scratching with a glass rod. Despite a 10 times higher concentration, the disappearance kinetics under MAS is only 4 times faster.

Figure S2 – Refocused INEPT spectra at the beginning of the MAS-induced sedimentation

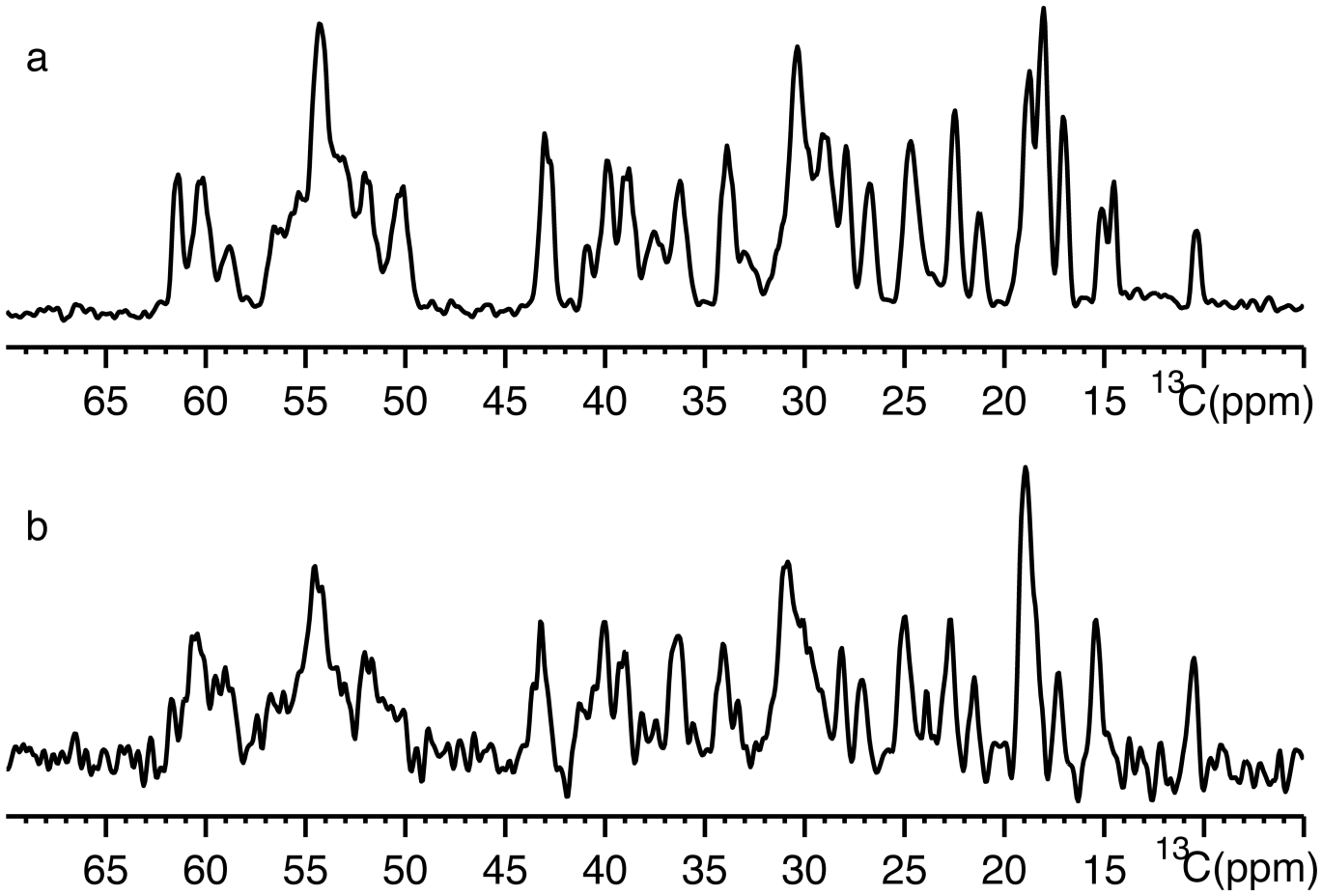

^{1}H-^{13}C Refocused INEPT spectra of the AβM40 (a) and of the sample of AβM42 (b) at the beginning of the MAS induced sedimentation experiment

Figure S3 – CP spectra of the AβM42 sample over the course of kinetics determination

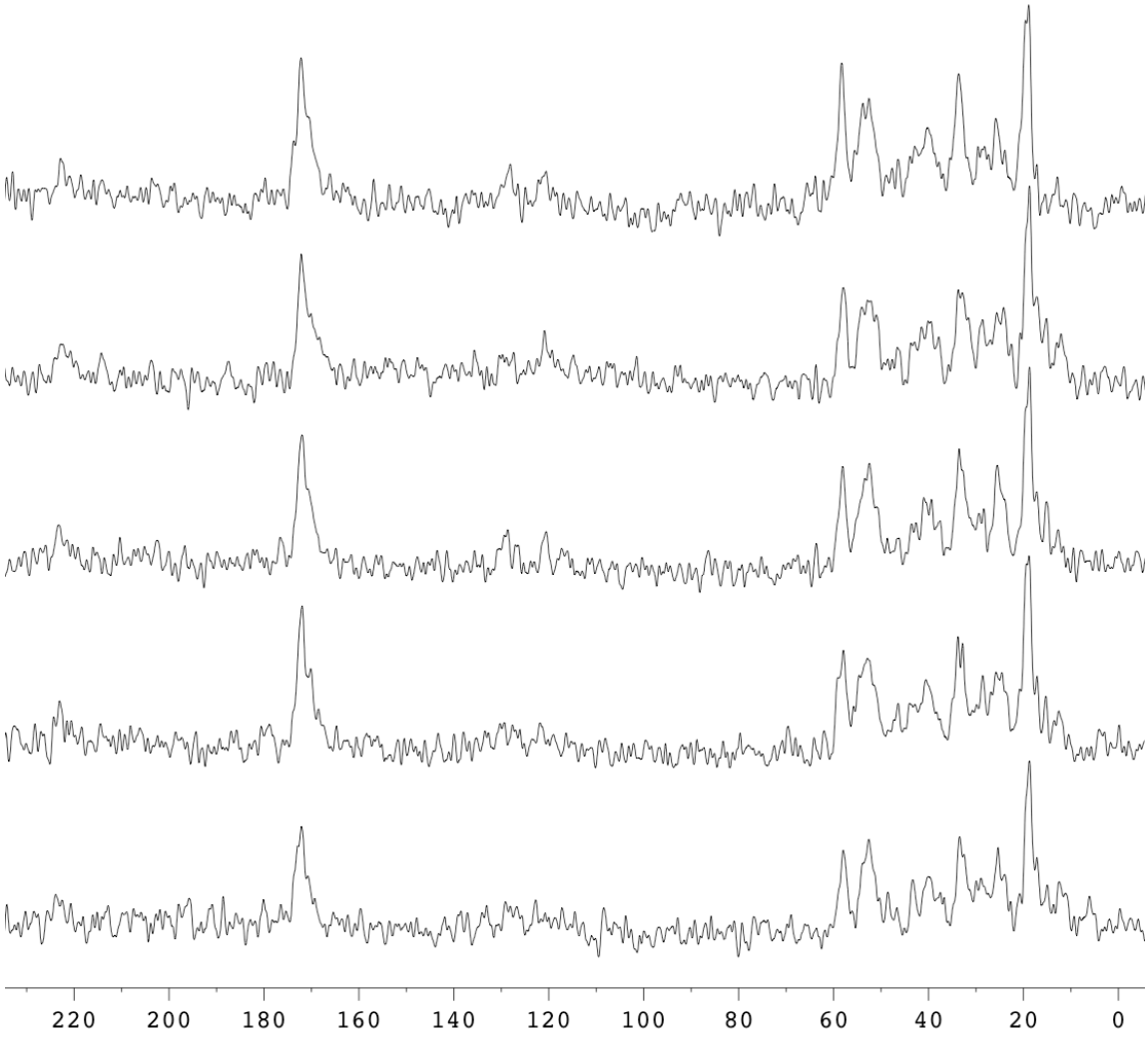

^{1}H-^{13}C CP spectra of the sample of AβM42 during the course of the kinetics determination *via* MAS induced sedimentation. From bottom to top experiments recorded at increasing time (1 h 49', 3 h 7', 4 h 25', 5 h 40', 7 h)

Figure S4 – NCO and NCA spectra of UC-1 sample

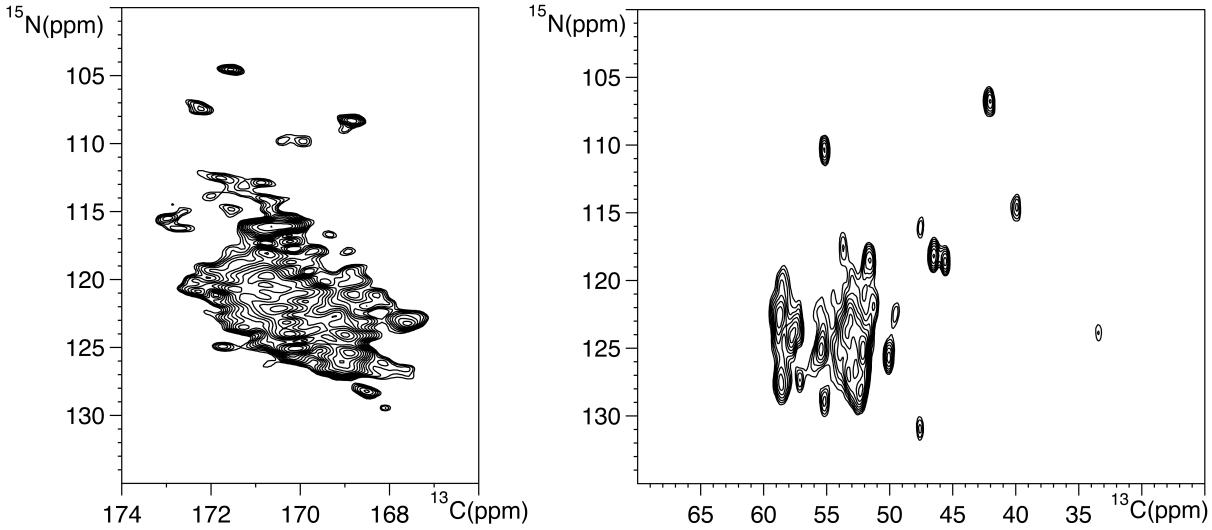

NCO (left) and NCA (right) spectra of UC-1 sample acquired at 700 MHz, 14 kHz spinning rate.

Figure S5 - Spectra of UC-2 and UC-3 samples

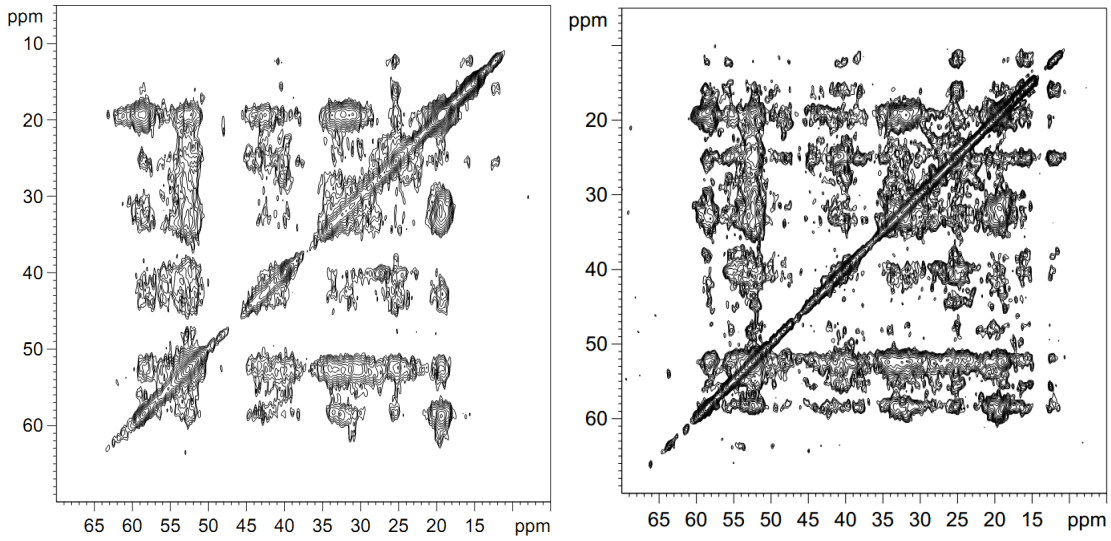

Representative 300 ms ^{13}C-^{13}C-SHANGHAI spectra of the preparations UC-2 and UC-3. UC-2 sample has higher initial concentration and the spectra suggest higher heterogeneity in the preparation. UC-3 should contain particles at higher molecular weight; the spectrum is more resolved than that of UC-2 but less resolved than that of UC-1, suggesting that longer time allows for formation of different species. It is noteworthy that and the number of crosspeaks in the spectrum of UC-3 is much larger than the corresponding spectrum of UC-1, suggesting that increased weight is accompanied by more compaction.

Figure S6 – Comparison of UC-1 and MAS-induced sediment spectra

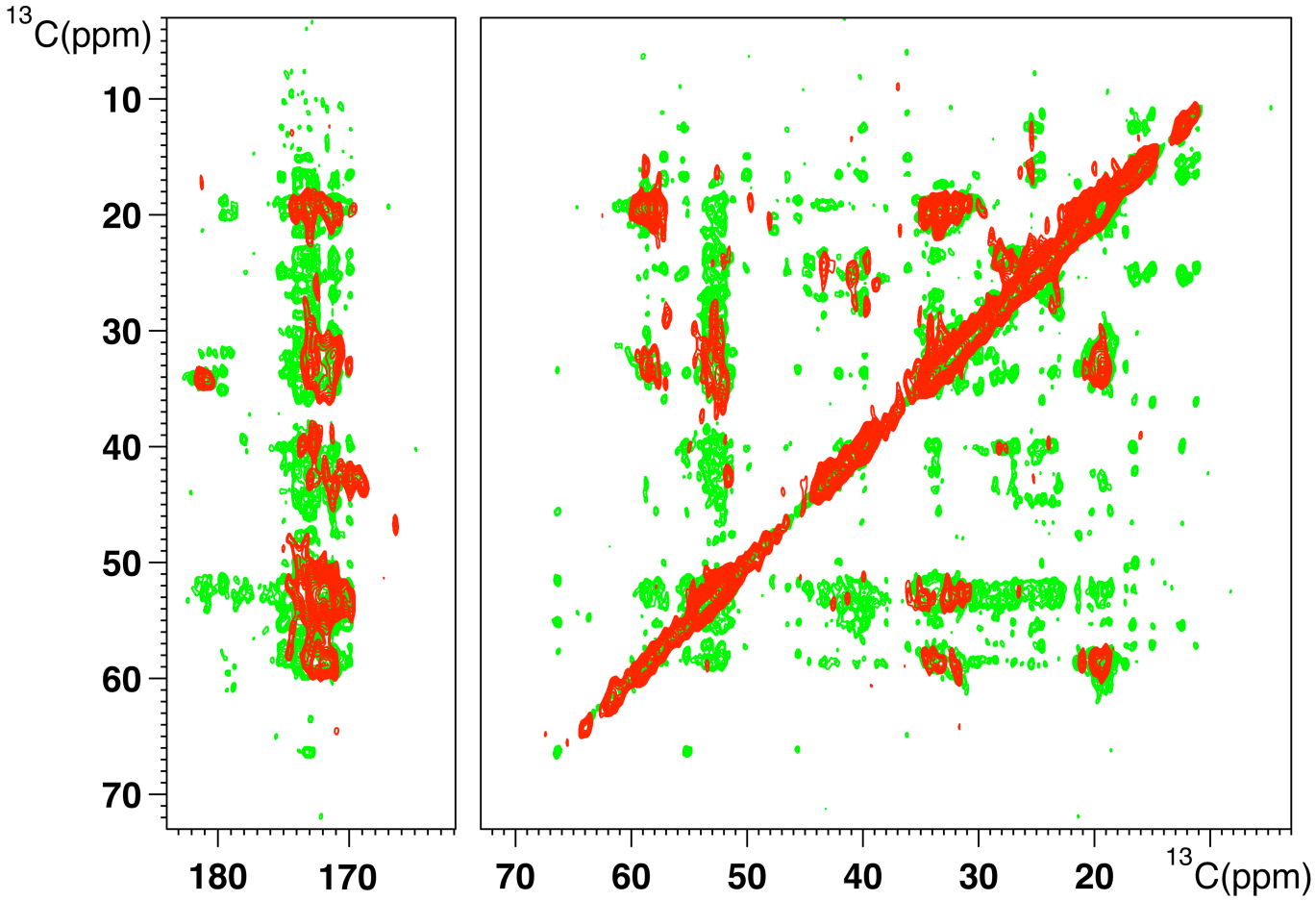

Overlay of 300 ms ^{13}C-^{13}C-SHANGHAI spectra of UC-1 sample (black) and MAS-induced sediment (red).

Figure S7 – Exemplification of the assignment strategy

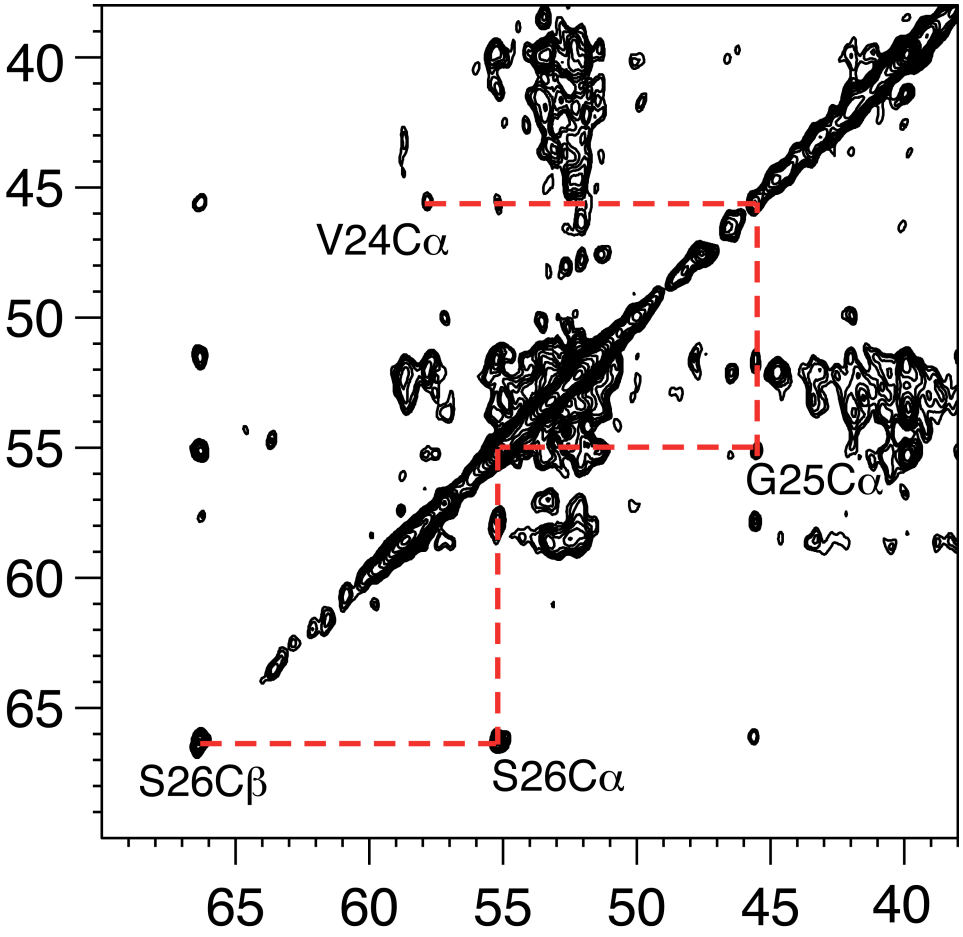

The figure indicates the approach that was followed to track sequential connectivity.

Figure S8 – Crosspeaks between E22 and K28

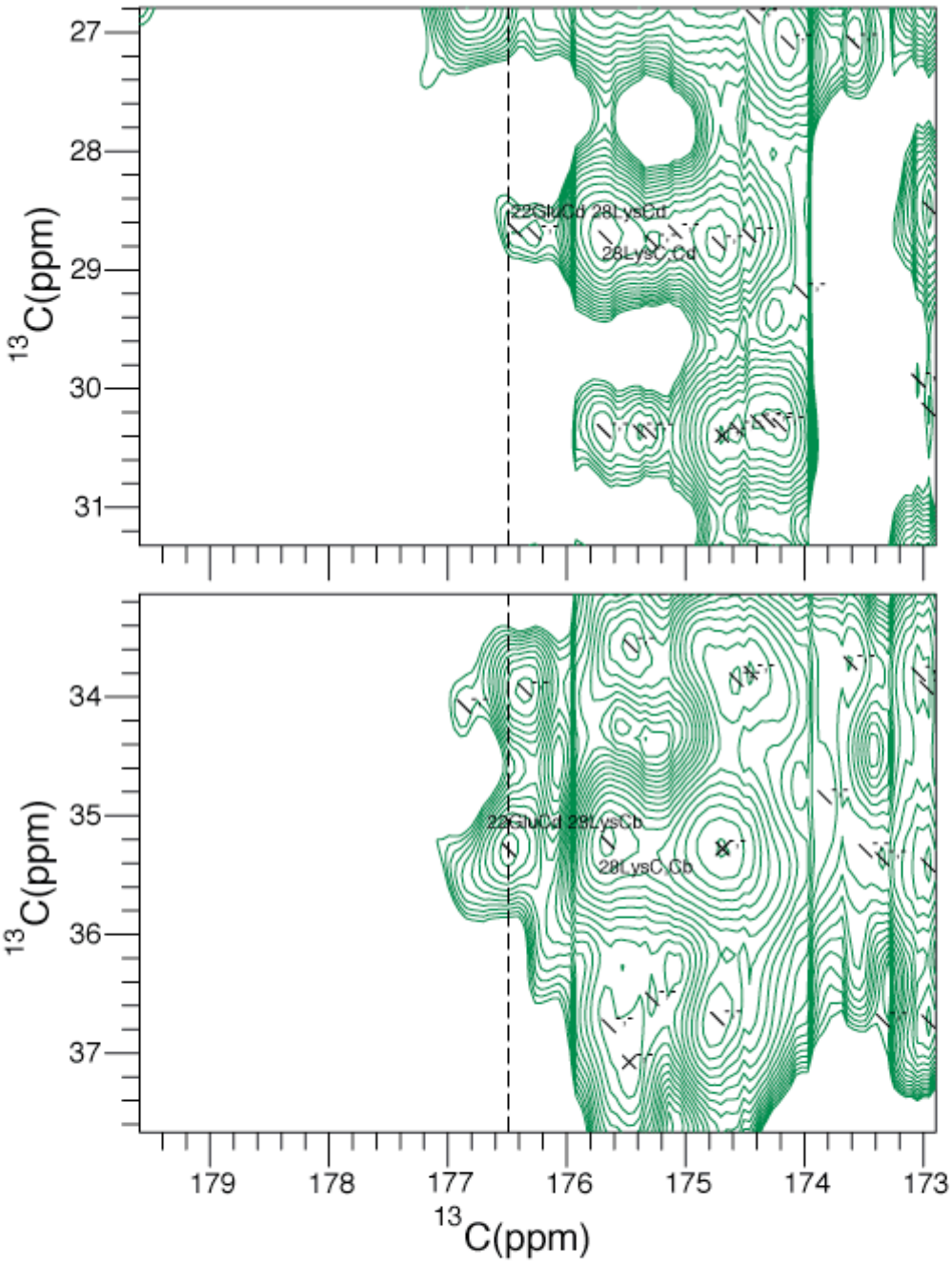

Enlargement of the carbonyl region in the 300 ms ^{13}C-^{13}C SHANGHAI spectrum of the UC1 sample, highlighting the crosspeaks between E22Cδ and carbon atoms from K28.

Figure S9 TALOS and PREDITOR secondary structure prediction

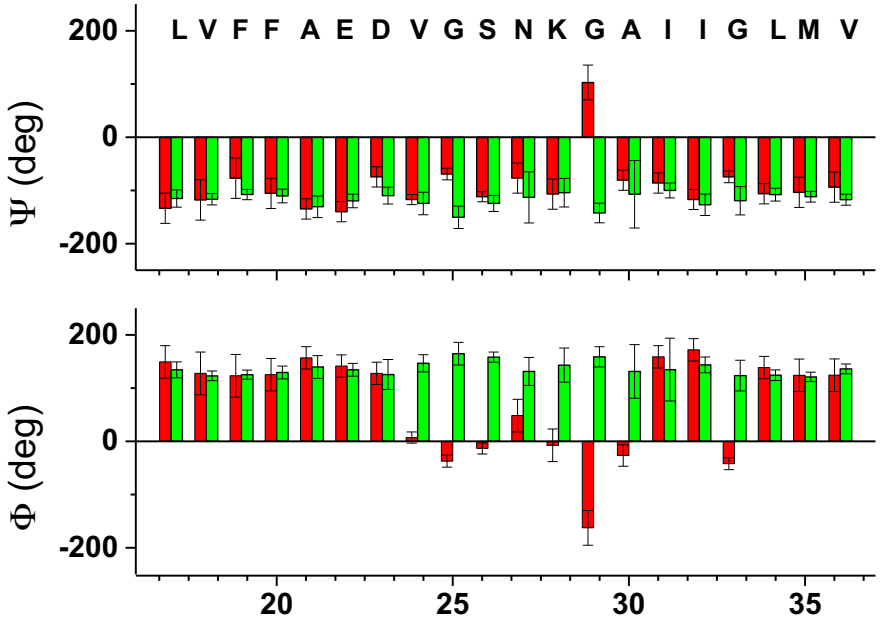

The figure reports the TALOS+ (green) and PREDITOR (red) estimates of the backbone dihedral angles.

Sedimentation in Solid State NMR rotors

The concentration profile of a single species in the centrifugal field induced by the Magic Angle Spinning of the solid state NMR rotor (i.e.: a cylinder spinning about its symmetry axis) is described by the following equation[3]:

$$c(r) = \frac{c_{\text{limit}}}{A\exp\left[-\frac{M(1-\bar{v}\rho)\omega_r^2 r^2}{2RT}\right]+1} \quad (1)$$

where A is analytically evaluated as:

$$A = \frac{\exp\left[\frac{M(1-\bar{v}\rho)\omega_r^2 b^2}{2RT}\left(1-\frac{c_0}{c_{\text{limit}}}\right)\right]-1}{1-\exp\left[-\frac{M(1-\bar{v}\rho)\omega_r^2 b^2}{2RT}\frac{c_0}{c_{\text{limit}}}\right]} \quad (2)$$

and the limiting concentration c_{limit} is experimentally found to be around 700 mg/ml[9;10].

From the results obtained for bullfrog apoferritin, we can estimate that the protein becomes rotationally immobilized at approximately 85% of this threshold value. The lowest MW for which enough material is sedimented is 69 kDa.

Data analysis and further considerations in kinetics determination via MAS induced sedimentation

Signal intensities of INEPT and CP of the AβM40 sample in figure 2 are obtained as normalized to the most intense signal of the respective series by Bruker Topspin 2.1. Successively they were multiplied by a factor 0.87, so that the sum of the last two points was 1, as obtained solving the following system:

$$\begin{cases} k'S(t_0) = x \\ k'S(t_{fin}) = 1 - y \\ kL(t_0) = 1 - x \\ kL(t_{fin}) = y \end{cases}$$

Where S is the solid-state CP signal and L is the liquid state INEPT signal (the same factor 0.87 was used for the AβM42 sample) at times t_0 and t_{fin}. This corresponds to the assumption that only two species are present in the sample at times t_0 and t_{fin}. As the two normalized curves sum to approximately 1 also at all intermediate times, no appreciable amounts of invisible intermediate species can be present (unless the invisible species is formed with the same kinetics of the visible one and is indefinitely stable). In addition to this, soluble oligomers up to >70 kDa should still be visible by INEPT, thus overlapping with the estimated MW of the sedimented species. This further excludes that invisible species may be present. This is not necessarily true for more diluted solutions or lower MAS rates, that would cause sedimentation starting from higher MW species that, when still in solution, may already have become invisible by INEPT. This could be the case for the AβM42 sample.

Clearing factor of a 4 mm Solid State NMR rotor

The clearing factor (K) with this kind of geometry cannot be evaluated according to the integrated Svedberg equation

$$t = \frac{K}{s} = \frac{\ln(r_{max}/r_{min})}{s\omega^2}\frac{10^{13}}{3600} (3),$$

since no "extra" gravity exists for the molecules in solution exactly at the axis of rotation (r_{min}=0), thus the required time would turn out to be infinite.

Anyway, even a minor movement of the center of mass out of the rotation axis will bring the protein into the centrifugal field, and the time required for the sediment NMR signal to appear can be used to estimate the clearing factor.

The time required for sedimenting a solution of bullfrog M apoferritin (17 S) at 12 kHz was measured to be 1.5 hours.

By its definition the clearing factor was calculated to be

$$K(12) = t(12)\cdot s = 1.5\cdot 17 \approx 26 \ (4)$$

and verified at 9 kHz

$$K(9) = K(12)\frac{12^2}{9^2} = 26\cdot 1.78 \approx 46 \ (5)$$

which corresponds to a sedimentation time at 9 kHz of

$$t(9) \approx \frac{46}{17} \approx 2.7h \ (6)$$

consistently with what experimentally determined.

Sedimentation in ultracentrifugal device and calculation of the sedimentation coefficients

The concentration profile of a single species in the ultracentrifugal device is described by equation 1, although in this case A cannot be obtained analytically[4] and must be evaluated by numerical integration of the equation:

$$\int_{r_{\min}}^{r_{\max}} S(r)c(r)\mathrm{d}r = c_0 V_{device} \quad (7)$$

where $S(r)$ is the area of the device at position r. In our experimental conditions (f = 32000 rpm, T = 4 °C) the minimum molecular weight for which sedimentation is obtained is about 20 kDa.

So, in this case, the smallest sedimentation coefficient of the species that sediment at the rotor can be estimated by equation 3, or, more conveniently, by the following equation:

$$s = \frac{K}{t} = \frac{\ln(r_{\max}/r_{\min})}{tf^2} 2.533 \cdot 10^{11} = \frac{\ln(134.7/89.50) \cdot 2.533 \cdot 10^{11}}{24 \cdot 1.024 \cdot 10^9} \approx 4.2S$$

From this value, according to the analysis performed by Fawzi et al.[29], a molecular mass of about 70 kDa can be calculated.

Table S1 -^{13}C chemical shifts of the assigned residues

Residue number	Residue type	CO	Cα	Cβ	Cγ	Cδ	Cε	N
16	Lys	172.7	53.9	33.8	26.5	28.6	41.2	128.9
17	Leu	173.9	53.57	46.29	28.41	25.58,19.00	-	124.9
18	Val	171.91	60.43	34.77	19.04,23.06	-	-	123.8
19	Phe	172.99	56.84	39.4	-	-	-	128.89
20	Phe	172.7	56.89	41.6	-	-	-	129.11
21	Ala	172.7	48.98	22.96	-	-	-	125.6
22	Glu	172.5	52.5	33.94	36.73	176.49	-	117.8
23	Asp	174.54	53.79	37.07	181.24	-	-	124.4
24	Val	174.6	59.35	34.92	20.39,21.90	-	-	123.1
25	Gly	172.86	47.22	-	-	-	-	110.4
26	Ser	174.61	56.79	67.9	-	-	-	110.55
27	Asn	172.8	53.05	35.82	182.59	-	-	116.4
28	Lys	175.54	55.24	35.35	25.24	28.55	41.61	128.2
29	Gly	171.7	43.54	-	-	-	-	105.4
30	Ala	175.57	51.66	18.18	-	-	-	122.3
31	Ile	174.83	58.8	37.83	16.73,26.23	12.93	-	120.6
32	Ile	176.85	57.01	41.7	18.39,26.73	14.19	-	124.4
33	Gly	171.6	48.13	-	-	-	-	115.5
34	Leu	172.93	53.84	45.14	30.28	28.69,24.82	-	127.6
35	Met	172.72	54.66	33.95	31.93	-	20.53	125
36	Val	176.71	60.04	32.4	20.41,21.97	-	-	125.7
37	Gly	170.62	40	-	-	-	-	
38	Gly	169	42.9	-	-	-	-	

Reference List

[1.] I. Bertini, C. Luchinat, G. Parigi, E. Ravera, B. Reif, P. Turano, *Proc.Natl.Acad.Sci.USA* **2011,** *108* 10396-10399.

[2.] T. Polenova, *Nature Chemistry* **2011,** 759-760.

[3.] I. Bertini, F. Engelke, C. Luchinat, G. Parigi, E. Ravera, C. Rosa, P. Turano, *Phys.Chem.Chem.Phys.* **2012,** *14* 439-447.

[4.] I. Bertini, F. Engelke, L. Gonnelli, B. Knott, C. Luchinat, D. Osen, E. Ravera, *J.Biomol.NMR* **2012,** *54* 123-127.

[5.] C. Gardiennet, A. K. Schütz, A. Hunkeler, B. Kunert, L. Terradot, A. Böckmann, B. H. Meier, *Angew.Chem.Int.Ed* **2012,** *51* 7855-7858.

[6.] E. Ravera, B. Corzilius, V. K. Michaelis, C. Rosa, R. G. Griffin, C. Luchinat, I. Bertini, *J.Am.Chem.Soc.* **2013,** *135* 1641-1644.

[7.] I. Bertini, C. Luchinat, G. Parigi, E. Ravera, *Acc.Chem.Res.* **2013,** *Epub ahead of print* .

[8.] Y. Wang, C. Li, G. J. Pielak, *JACS* **2010,** *132* 9392-9397.

[9.] S. Lundh, *Archives of Biochemistry and Biophysics* **1985,** *241* 265-274.

[10.] S. Lundh, *Journal of Polymer Science: Polymer Physics Edition* **1980,** *18* 1963-1978.

[11.] A. Böckmann, C. Gardiennet, R. Verel, A. Hunkeler, A. Loquet, G. Pintacuda, L. Emsley, B. H. Meier, A. Lesage, *J.Biomol.NMR* **2009,** *45* 319-327.

[12.] A. J. Baldwin, P. Walsh, D. F. Hansen, G. R. Hilton, J. L. P. Benesch, S. Sharpe, L. E. Kay, *J.Am.Chem.Soc.* **2012,** *134* 15343-15350.

[13.] A. Mainz, B. Bardiaux, F. Kuppler, G. Multhaup, I. C. Felli, R. Pierattelli, B. Reif, *J.Biol.Chem.* **2012,** *287* 1128-1138.

[14.] N. Carulla, M. Zhou, E. Giralt, C. V. Robinson, C. M. Dobson, *Acc.Chem.Res.* **2010,** *43* 1072-1079.

[15.] H. A. Scheidt, I. Morgado, S. Rothemund, D. Huster, M. Fandrich, *Angew.Chem.Int.Ed.* **2011,** *50* 2837-2840.

[16.] I. Benilova, E. Karran, B. De Strooper, *Nat.Neurosci.* **2012,** *15* 1-9.

[17.] S. L. Gallion, *Plos ONE* **2012,** *7* e49375.

[18.] R. Roychaudhuri, M. Yang, M. M. Hoshi, D. B. Teplow, *J.Biol.Chem.* **2009,** *284* 4749-4753.

[19.] G. Bitan, S. S. Vollers, D. B. Teplow, *J.Biol.Chem.* **2003,** *278* 34882-34889.

[20.] S. L. Bernstein, N. F. Dupuis, N. D. Lazo, T. Wyttenbach, M. M. Condron, G. Bitan, D. B. Teplow, J. E. Shea, B. T. Ruotolo, C. V. Robinson, M. T. Bowers, *Nature Chem.* **2009,** *1* 326-331.

[21.] M. Fandrich, M. Schmidt, N. Grigorieff, *Trends in Biochemical Sciences* **2011,** *36* 338-345.

[22.] R. Tycko, *Annu.Rev.Phys.Chem.* **2011,** *62* x-xx.

[23.] I. Bertini, L. Gonnelli, C. Luchinat, J. Mao, A. Nesi, *J.Am.Chem.Soc.* **2011,** *133* 16013-16022.

[24.] J. M. Lopez del Amo, M. Schmidt, U. Fink, M. Dasari, M. Fändrich, B. Reif, *Angew.Chem Int.Ed Engl.* **2012,** *51* 6136-6139.

[25.] S. Chimon, Y. Ishii, *J.Am.Chem.Soc.* **2005,** *127* 13472-13473.

[26.] J. Danielsson, A. Andersson, J. Jarvet, A. Gräslund, *Magn Reson.Chem.* **2006,** *44* S114-S121.

[27.] I. Kheterpal, M. Chen, K. D. Cook, R. Wetzel, *J.Mol.Biol.* **2006,** *361* 785-795.

[28.] M. Ahmed, J. Davis, D. Aucoin, T. Sato, S. Ahuja, S. Aimoto, J. I. Elliott, W. E. Van Nostrand, S. O. Smith, *Nat.Struct.Mol.Biol.* **2010,** *17* 561-567.

[29.] N. L. Fawzi, J. Ying, R. Ghirlando, D. A. Torchia, G. M. Clore, *Nature* **2011,** *480* 268-272.

[30.] J. Pan, J. Han, C. H. Borchers, L. Konermann, *Anal.Chem.* **2011,** *83* 5386-5393.

[31.] M. Fandrich, *J Mol.Biol.* **2012,** *421* 440.

[32.] C. Haupt, J. Leppert, R. Rönicke, J. Meinhardt, J. K. Yadav, R. Ramachandran, O. Ohlenschläger, K. G. Reymann, M. Görlach, M. Fandrich, *Angew.Chem Int.Ed Engl.* **2012,** *51* 1576-1579.

[33.] J. Bieschke, M. Herbst, T. Wiglenda, R. P. Friedrich, A. Boeddrich, F. Schiele, D. Kleckers, J. M. Lopez del Amo, B. A. Grüning, Q. Wang, M. R. Schmidt, R. Lurz, R. Anwyl, S. Schnoegl, M. Fandrich, R. F. Frank, B. Reif, S. Günther, D. M. Walsh, E. E. Wanker, *Nat.Chem.Biol.* **2012,** *8* 93-101.

[34.] J. M. Lopez del Amo, U. Fink, M. Dasari, G. Grelle, E. E. Wanker, J. Bieschke, B. Reif, *J.Mol.Biol.* **2012,** *421* 517-524.

[35.] J. C. Stroud, L. Cong, P. K. Teng, D. Eisenberg, *Proc.Natl.Acad.Sci.USA* **2012,** *109* 7717-7722.

[36.] M. D. Kirkitadze, G. Bitan, D. B. Teplow, *J.of Neurosci.Res.* **2002,** *69* 567-577.

[37.] J. Lee, E. K. Culyba, E. T. Powers, J. W. Kelly, *Nat.Chem.Biol.* **2011,** *7* 602-609.

[38.] P. Schanda, E. Kupce, B. Brutscher, *J.Biomol.NMR* **2005,** *33* 199-211.

[39.] K. Pauwels, T. L. Williams, K. L. Morris, W. Jonkheere, A. Vandersteen, G. Kelly, J. Schymkowitz, F. Rousseau, A. Pastore, L. C. Serpell, K. Broersen, *J.Biol.Chem.* **2012,** *287* 5650-5660.

[40.] G. A. Morris, R. Freeman, *J.Am.Chem.Soc.* **1979,** *101* 760-762.

[41.] W. Bermel, I. Bertini, I. C. Felli, M. Piccioli, R. Pierattelli, *Progr.NMR Spectrosc.* **2006,** *48* 25-45.

[42.] R. Riek, G. Wider, K. Pervushin, K. Wüthrich, *Proc.Natl.Acad.Sci.USA* **1999,** *96* 4918-4923.

[43.] A. Pines, M. G. Gibby, J. S. Waugh, *J Chem Phys* **1972,** *56* 1776-1777.

[44.] A. Mainz, S. Jehle, B. J. van Rossum, H. Oschkinat, B. Reif, *J.Am.Chem.Soc.* **2009,** *131* 15968-15969.

[45.] W. B. Jr. Stine, K. N. Dahlgren, G. A. Krafft, LaDu M.J., *J Biol.Chem.* **2003,** *278* 11612-11622.

[46.] I. Kuperstein, K. Broersen, I. Benilova, J. Rozenski, W. Jonekheere, M. Debulpaep, A. Vandersteen, I. Segers-Nolten, K. Van der Werf, V. Subramaniam, D. Braeken, G. Callewaert, C. Bartic, R. D'Hooge, I. C. Martins, F. Rousseau, J. Schymkowitz, B. De Strooper, *EMBO J.* **2010,** *29* 3408-3420.

[47.] R. C. Chatelier, A. P. Minton, *Biopolymers* **1987,** *26* 507-524.

[48.] A. T. Petkova, R. D. Leapman, Z. H. Guo, W. M. Yau, M. P. Mattson, R. Tycko, *Science* **2005,** *307* 262-265.

[49.] A. K. Paravastu, R. D. Leapman, W. M. Yau, R. Tycko, *Proc.Natl.Acad.Sci.USA* **2008,** *105* 18349-18354.

[50.] R. J. Ellis, A. P. Minton, *Biological Chemistry* **2006,** *387* 485-497.

[51.] D. A. White, A. K. Buell, T. P. J. Knowles, M. E. Welland, C. M. Dobson, *J.Am.Chem.Soc.* **2010,** *132* 5170-5175.

[52.] A. Magno, A. Caflisch, R. Pellarin, *J.Phys.Chem.Lett.* **2010,** *1* 3027-3032.

[53.] T. P. J. Knowles, C. A. Waudby, G. L. Devlin, S. I. A. Cohen, A. Aguzzi, M. Vendruscolo, E. M. Terentjev, M. E. Welland, C. M. Dobson, *Science* **2009,** *326* 1533-1537.

[54.] H.-Y. Kim, M.-K. Cho, A. Kumar, E. Maier, C. Siebenhaar, S. Becker, C. O. Fernandez, H. A. Lashuel, R. Benz, A. Lange, M. Zweckstetter, *J.Am.Chem.Soc.* **2009,** *131* 17482-17489.

[55.] Y. F. Mok, G. J. Howlett, *Methods In Enzymology* **2006,** *413* 199-217.

[56.] D. Kashchiev, R. Cabriolu, S. Auer, *J.Am.Chem.Soc.* **2013,** *135* 1531-1539.

[57.] B. Hu, O. T. J. Lafon, Q. Chen, J.-P. Amoureux, *Journal of Magnetic Resonance* **2011,** *212* 320-329.

[58.] N. M. Loening, M. Bjerring, N. C. Nielsen, H. Oschkinat, *Journal of Magnetic Resonance* **2012,** *214* 81-90.

[59.] A. Sandberg, L. M. Luheshi, S. Sollvander, T. P. de Barros, B. Macao, T. P. J. Knowles, H. Biverstal, C. Lendel, F. Ekholm-Petterson, A. Dubnovitsky, L. Lannfelt, C. M. Dobson, T. Hard, *Proceedings of the National Academy of Sciences of the United States of America* **2010,** *107* 15595-15600.

[60.] M. V. Berjanskii, S. Neal, D. S. Wishart, *Nucleic Acids Res.* **2006,** *34* W63-W69.

[61.] Y. Shen, F. Delaglio, G. Cornilescu, A. Bax, *Journal of Biomolecular NMR* **2009,** *44* 213-223.

[62.] T. A. Wassenaar, M. van Dijk, N. Loureiro-Ferreira, G. van der Schot, S. J. de Vries, C. Schmitz, J. van der Zwan, R. Boelens, A. Giachetti, L. Ferella, A. Rosato, I. Bertini, T. Herrmann, H. R. A. Jonker, A. Bagaria, V. Jaravine, P. Guntert, H. Schwalbe, W. F. Vranken, J. F. Doreleijers, G. Vriend, G. W. Vuister, D. Franke, A. Kikhney, D. I. Svergun, R. H. Fogh, J. Ionides, E. D. Laue, C. Spronk, S. Jurksa, M. Verlato, S. Badoer, S. Dal Pra, M. Mazzucato, E. Frizziero, A. M. J. J. Bonvin, *Journal of Grid Computing* **2012,** *10* 743-767.

[63.] S. Chimon, M. A. Shaibat, C. R. Jones, D. C. Calero, B. Aizezi, Y. Ishii, *Nature Structural & Molecular Biology* **2007,** *14* 1157-1164.

[64.] A. T. Petkova, W. M. Yau, R. Tycko, *Biochemistry* **2006,** *45* 498-512.